Thanh, V. H.; Okubo, K.; Shibasaki, K. Isolation and Characterization of the Multiple 7S Globulins of Soybean Proteins. *Plant Physiol.* **1975**, *56*, 19.
Trewhella, J.; Appleby, C. A.; Wright, P. E. Proton NMR studies of high-spin complexes of soy leghemoglobin. Interactions between the distal histidine and acetate, formate and fluoride ligands. *Aust. J. Chem.* **1986**, *39* (2), 317-24.
Wright, D. J. The Seed Globulins. In *Developments in Food Proteins - 5*; Hudson, B. J. F., Ed.; Elsevier Applied Science: London, New York, 1976; pp 81-157.
Wüthrich, K. Carbon-13 NMR of Amino Acids, Peptides and Proteins. In *NMR Biological Research: Peptides and Proteins*; North Holland/American Elsevier: Amsterdam, Oxford, New York, 1976.
Yamauchi, F.; Yamagishi, Y. Carbohydrate Sequence of a Soybean 7S Protein. *Agric. Biol. Chem.* **1979**, *43* (3), 505-10.
Yamauchi, F.; Ono, H.; Kamata, Y.; Shibasaki, K. Acetylation of Amino Groups and Its Effect on the Structure of Soybean Glycinin. *Agric. Biol. Chem.* **1979**, *43* (6), 1309-15.

Received for review November 15, 1988. Revised manuscript received August 29, 1989. Accepted December 14, 1989.

# Carbon-13 NMR Studies of the Effects of Gelation and Heat and Chemical Denaturation at Neutral pH on Soy Glycinin and β-Conglycinin

Michael S. Fisher, Wayne E. Marshall,* and Henry F. Marshall, Jr.

Southern Regional Research Center, USDA—ARS, P.O. Box 19687, New Orleans, Louisiana 70179

Carbon-13 NMR studies have been carried out on soy glycinin and β-conglycinin under conditions of gelation and heat and chemical denaturation in pH 7.0 aqueous solutions containing 0.035 M phosphate and 0.4 M NaCl. With 6 M urea as a chemical denaturant, major changes were seen in the appearance of the aliphatic and aromatic carbon regions of the protein spectra, particularly in that of β-conglycinin. However, carbon chemical shifts underwent little or no change during denaturation, confirming that the sharp peaks observed in the native proteins were largely from mobile groups in random regions. As the temperature of the protein solutions was increased, many additional peaks were observed, especially in β-conglycinin, and existing peaks in both proteins became sharper, consistent with increased molecular motion and protein unfolding. Upon gelation, both protein gels gave spectra consistent with involvement of aliphatic and aromatic amino acids in gel structure. The β-conglycinin gel also showed evidence of the involvement of the carbohydrate and glutamate side chains in gel structure. The data support the concept that gelation of both proteins is a four-step process involving (1) unfolding (different from denaturation), (2) aggregation, (3) strand formation, and (4) strand ordering/gelation.

Although $^{13}C$ NMR has been used to study a number of food proteins (Baianu, 1989), some at elevated temperature (Belton et al., 1987; Baianu et al., 1982), the effects of heat and chemical denaturation and gel formation of purified soy proteins has hitherto not been studied by NMR. Hermansson (1978) and Koshiyama et al. (1981) have reported the denaturation temperature for soy 7S and 11S proteins and studied turbidity changes during the denaturation-gelation process. Suresh Chandra et al. (1984) used circular dichroism and optical rotatory dispersion to determine the effects of temperature on the secondary and tertiary structures of glycinin. They found no change in the native structure over the temperature range 15-60 °C. However, in the presence of urea or guanidine hydrochloride denaturant, a disordered structure was observed at 15 °C that appeared to become more ordered at higher temperatures. The highest temperature used by Suresh Chandra et al. (1984) was 60 °C, below the denaturation temperature for both glycinin and β-conglycinin (Hermansson, 1978). Dev et al. (1988) have studied changes in glycinin conformation upon urea and heat denaturation with FT-IR.

Both glycinin and β-conglycinin can form self-supporting gels upon heating. When glycinin is heated to 95 °C in the presence of sodium chloride, the gel structure is dominated by ordered strands rather than disordered aggregates; β-conglycinin produces a somewhat less ordered gel matrix after being heated to 85 °C (Hermansson, 1986). Gel formation occurs at concentrations above 2.5% and 7.5% for glycinin and β-conglycinin, respectively (Nakamura et al., 1986a). To date, structural studies of soy storage protein gels have used electron microscopy (Hermansson, 1985, 1986; Mori et al., 1986), electrophoresis, gel immunodiffusion, and other methods (Utsumi and Kinsella, 1985; Nakamura et al., 1986a,b). The methods used by these workers precluded actual observation of protein behavior at particular temperatures. Their methods supply only limited information on specific types of amino acids that may be involved in maintaining gel structure and are limited in their inability to observe pro-

tein conformation at elevated temperatures.

Both a previous NMR study of soy proteins (Kakalis and Baianu, 1985) and an earlier study of ours (Fisher et al., 1990) focused on the $^{13}C$ NMR spectra of undenatured materials. A third study (Baianu, 1989) on soy protein isolates was done at elevated pHs and on hydrolysates at very low pH. Using a phosphate–NaCl medium at room temperature and pH 7.0, Fisher et al. (1990) made peak assignments for most of the amino acids and similarities and differences in protein structure between the two soy storage proteins were discussed. The objective of the present study is to extend this earlier work, determine the effects of gelation and heat and chemical denaturation on the $^{13}C$ NMR characteristics of glycinin and β-conglycinin structure, and directly observe glycinin and β-conglycinin conformation at elevated temperatures by carbon-13 NMR spectroscopy.

## PROCEDURE

**Protein Isolation and Purification.** Crude glycinin was prepared from Nutrasoy 7B flakes (Archer Daniels Midland Co., Decatur, IL) by a modification of the procedure of Thanh et al. (1975), which is based on the differential solubility of β-conglycinin and glycinin in 0.063 M Tris buffer (pH 6.6) containing 0.010 M 2-mercaptoethanol (2-ME). Soy flakes were dispersed in 0.063 M Tris buffer (pH 7.8) containing 0.010 M 2-ME (1:15 ratio). The suspension was extracted for 2 h at ambient temperature and centrifuged for 30 min at 10000*g* and the precipitate discarded. The resulting supernatant was filtered through a 0.22-μm Millipore filter and then exhaustively dialyzed against water at 4 °C. The retentate was centrifuged for 30 min at 10000*g*. The precipitate was suspended in deionized water and lyophilized. The crude glycinin (750-mg portions) was dispersed in pH 7.6 0.035 M phosphate buffer containing 0.4 M NaCl and 0.010 M 2-ME and then fractionated on a 2.5 × 80 cm column of Sepharose 6B with a flow rate of 25 mL/min. Purity of the preparation was ascertained by lithium dodecyl sulfate–polyacrylamide gel electrophoresis using the procedures outlined by Laemmli (1970). The remaining column eluate was dialyzed against water and lyophilized. Glycinin prepared in this manner was approximately 93% pure and was used without further purification.

β-Conglycinin was prepared by Walter J. Wolf (Northern Regional Research Center, USDA—ARS, Peoria, IL) using a modification of the procedure of Thanh and Shibasaki (1976). In it, the initial extraction was made with 0.03 M Tris-HCl containing 0.005 M ethylenediaminetetraacetic acid (EDTA). The crude β-conglycinin was purified by dissolving 2 g in 25 mL of pH 7.6 0.5 ionic strength phosphate–NaCl buffer containing 0.01 M 2-ME and 0.01% Thimerosol and pumping it through a 2.6 × 13 cm column of Concanavalin A–Sepharose 4B. The β-conglycinin was eluted with a gradient from 0 to 0.5 M of methyl α-D-glucoside. Samples, assayed for purity by Dr. Wolf by ultracentrifugation, were combined to yield a spectrometric sample containing approximately 92% β-conglycinin and 8% glycinin.

**Protein Denaturation.** Protein samples were dissolved in an aqueous buffer containing 30% $D_2O$, 0.035 M potassium phosphate, 0.4 M NaCl, and 6 M urea and the mixtures adjusted to pH 7.0. The final protein concentrations were 100 mg/mL. Spectra were obtained at 25 °C.

**Formation of Protein Gels.** Protein solutions, in the absence of urea, were heated in the NMR probe to the lowest desired temperature, and data acquisition was initiated. At the conclusion of data acquisition, the temperature was raised to the next higher temperature and acquisition restarted. This process was repeated to the highest obtained temperature for each sample. The glycinin sample heated to 95 °C and the β-conglycinin sample heated to 85 °C were cooled to 4 °C immediately after removal from the NMR probe in order to promote gel formation. NMR spectra of the gels were subsequently obtained at 25 °C.

**NMR Methods.** All samples were measured as 100 mg/mL solutions in an aqueous buffer containing 30% $D_2O$, 0.035 M potassium phosphate, and 0.40 M sodium chloride and the mixtures adjusted to pH 7.0. Solvent was filtered through piggyback 0.45- and 0.22-μm filters to remove fungal and bacterial contaminants. Tubes were washed with 95% ethanol and acetone and dried at 110 °C. In samples treated this way, the obvious results of decomposition (e.g., foul odor) did not appear until after 10 days of storage in solution at room temperature. Acetonitrile (0.25%) was used as an internal reference (chemical shift at pH 7.0 (25 °C) 1.30 and 119.61 ppm).

All spectra were obtained with a Varian VXR-200 spectrometer using a 10-mm sample tube containing 3 mL of solution and 0.30 g of protein. Spectra were acquired at 50.309 MHz over a spectral width of 11 148.3 Hz and proton-decoupled with the WALTZ sequence (Shaka et al., 1983) using 256-pulse blocks, each block preceded by a four-pulse steady-state sequence. Recycle time was 0.6 s; tip angle was 62.5°. Fourier transforms were done on 13 376 points, zero-filled to 16 384, and processed with 5-Hz exponential line broadening and 0.05-s Gaussian apodization ($\exp(-t^2/0.0025)$). To distinguish between close peaks, lines were converted from Lorentzian line shape to Gaussian line shape by weighting the free induction decays (FIDs) with combined exponential ($e^{t/s}$) and Gaussian functions. To emphasize narrow peaks, normal spectra were converted to convolution difference spectra by weighting the FIDs with the function $(1 - (0.9 \exp(-t/0.03)))$. Bandwidths were obtained with Varian-supplied software.

## RESULTS AND DISCUSSION

**General Considerations.** Chemical shift, peak assignment, and bandwidth data are presented as Tables I–III. Peak assignments were made based on those in the companion paper (Fisher et al., 1990) and literature values (Howarth and Lilley, 1978; Wüthrich, 1976; Kakalis and Baianu, 1989), aided by convolution difference and resolution enhancement weighting of the free induction decays as stated in NMR Methods. In several instances, most notably the 10–22 ppm region of β-conglycinin at 25 °C (Figures 1A and 3A; Tables I and III), assignment of peaks (Fisher et al., 1990) that could not be observed in the normal NMR spectrum were made with use of the APT sequence (Patt and Shoolery, 1982). Bandwidths were determined with the software available on the NMR instrument. Unreliable bandwidths resulted when accurate base line or half-height could not be determined by the software due to peak overlap. All bandwidths reported by the instrument to be unreliable were rejected.

Glycinin is a hexameric protein with an approximate molecular weight of 360 000. Each of its six subunits consists of a pair of polypeptide chains, made up of an acidic and a basic polypeptide connected by one or more disulfide linkages (Nielsen, 1985). Glycinin's secondary structure is roughly 20% α-helix, 17% β-structure, and 63% random coil (Ishino and Kudo, 1980). β-Conglycinin is a trimeric glycoprotein of molecular weight 180 000. It is reported to be 20% α-helix, 23% β-structure, and 57% random coil (Ishino and Kudo, 1980) and to contain about 5% carbohydrate (Koshiyama, 1968), composed of mannose and *N*-acetylglucosamine (Yamauchi and Yamagishi, 1979).

**Influence of Chemical Denaturation.** The $^{13}C$ NMR spectra of glycinin and β-conglycinin (Figure 1A,C) show areas (envelopes) where the apparent base line deviates significantly from the true spectral base line. These envelopes contain large numbers of peaks whose slight differences in chemical shift result from structured regions within the proteins. Peaks in structured regions are broadened by $T_2$-dominated relaxation (i.e., $T_2 \ll$ spin–lattice relaxation, $T_1$) resulting from the restricted motion in such regions. Thus, in general, the regions within the protein that are highly structured, whether α-helical, β-sheet, or random, yield spectra that are difficult to assign, even with pulse sequences such as APT. Qualitative gross struc-

**Table I. Room-Temperature and Denatured Glycinin and β-Conglycinin Peak Positions, Assignments, and Bandwidths**

| | glycinin | | | | β-conglycinin | | | |
|---|---|---|---|---|---|---|---|---|
| | −6 M urea | | +6 M urea | | −6 M urea | | +6 M urea | |
| peak assignment | ppm[a] | bw[b] | ppm | bw | ppm | bw | ppm | bw |
| Glu Cδ | 181.6 | 26.2 | 181.5 | 24.2 | 181.5 | 363.1 | 181.5 | 80.4 |
| Gln Cδ | 178.0 | 38.6 | 178.0 | 33.1 | 178.0 | c | 177.9 | 33.4 |
| C=O + Asn Cγ | 173.6 | 97.1 | 174.6 | 170.7 | 174.0 | 89.0 | 173.8 | 95.0 |
| C=O | d | | 173.9 | 111.2 | 172.4 | 221.2 | 172.3 | 191.3 |
| C=O | 172.1 | 215.0 | 172.3 | 205.6 | 172.0 | 220.8 | e | |
| Arg Cζ | 157.2 | 20.8 | 157.2 | 20.0 | 157.1 | 22.9 | 157.2 | 22.0 |
| Tyr Cζ | 154.8 | 50.6 | 155.0 | 40.5 | d | | 155.1 | 31.3 |
| Phe Cγ | 136.5 | c | 136.6 | 44.4 | 136.5 | 34.4 | 136.6 | 26.3 |
| His Cγ + Cε + His$^+$ Cγ | 135.2 | 40.5 | 136.6 | 143.8 | 135.6 | c | 134.7 | 65.3 |
| Tyr 2Cδ | 131.1 | 225.5 | 131.0 | 34.0 | 131.1 | 257.9 | 130.9 | 35.9 |
| Phe 2Cδ + His$^+$ Cε | 129.5 | 62.4 | 129.6 | 49.2 | 129.6 | 111.6 | 129.5 | 47.9 |
| Phe 2Cε | 129.1 | 68.4 | 129.2 | 52.9 | 129.0 | 113.0 | 129.1 | 48.8 |
| His$^+$ Cε | 128.5 | 227.3 | 128.0 | 68.2 | f | | d | |
| Phe Cζ + Tyr Cγ + Trp Cδ2[h] | 127.5 | 247.4 | 127.6 | 219.2 | 127.3 | 245.7 | 127.5 | 152.8 |
| Trp Cη[h] | 122.3 | 94.4 | 122.4 | 31.0 | e | | e | |
| His+ Cδ (+Trp Cε)[h] | 118.9 | 23.9 | 118.9 | 177.4 | f | | 118.9 | 88.0 |
| His Cδ (+Trp Cζ$_2$)[h] | 117.6 | 40.4 | 117.8 | 49.0 | 118.3 | 69.7 | 117.5 | 59.0 |
| Tyr 2Cε | 115.8 | 39.0 | 115.9 | 38.7 | 115.8 | 23.0 | 115.9 | 23.2 |
| Trp Cζ1[h] | d | | 112.3 | 14.5 | e | | e | |
| α-Man C1[g] | | | | | 102.6 | 26.0 | 102.6 | 15.4 |
| GlcNAc(Asn) C1[g] | | | | | 101.2 | 44.1 | 100.9 | 34.0 |
| GlcNAc(Asn) C2[g] | | | | | 78.7 | 50.4 | 78.8 | 26.2 |
| α-Man C5[g] | | | | | 73.5 | c | 73.8 | 23.1 |
| α-Man C2, C3, C4[g] | | | | | 70.5 | 94.2 | 70.5 | 35.6 |
| Thr Cβ (+β-Man C4, C6)[g] | 68.2 | 45.9 | 67.6 | 27.4 | 67.2 | c | 67.4 | 36.5 |
| Ser Cβ + (+α-Man C6)[g] | 61.4 | 171.6 | 61.7 | 67.6 | 61.5 | 99.5 | 61.6 | 62.6 |
| *trans*-Pro Cα (+GlcNAc(Asn) C2)[g] | 60.9 | c | 61.0 | 173.0 | 60.7 | 383.4 | 60.9 | 171.6 |
| *cis*-Pro Cα | f | | 60.1 | 179.9 | f | | 60.0 | 187.2 |
| Cα Env | 59.6 | c | 59.3 | 187.1 | f | | f | |
| Cα Env | 57.6 | c | 57.6 | 408.3 | f | | f | |
| Ser Cα (+GlcNAc(α-Man) C2)[g] | 55.9 | c | 56.0 | 166.5 | f | | f | |
| | | | | | 56.2 | 118.1 | 56.0 | 244.3 |
| Cα Env | f | | 55.2 | 263.0 | 55.9 | c | 55.9 | 266.1 |
| Cα Env | 53.9 | 105.0 | 54.1 | 72.9 | 54.1 | 85.3 | 54.2 | 68.7 |
| Asn Cα | 52.0 | 307.8 | 52.1 | 265.1 | 52.1 | c | 54.2 | 68.7 |
| Pro Cδ | 48.0 | c | 48.3 | 42.5 | 48.3 | c | 48.3 | 42.5 |
| Gly Cα | 42.9 | c | 43.0 | 37.2 | 42.9 | c | 43.0 | 47.0 |
| Gly Cα | 42.9 | c | 43.0 | 37.2 | 42.9 | c | 43.0 | 47.0 |
| Lys Cε + Arg Cδ | 41.0 | 144.6 | 41.2 | 31.2 | 41.0 | 115.4 | 41.1 | 28.6 |
| Asp Cβ + Asn Cβ | 39.6 | 40.2 | 39.8 | 55.7 | 39.7 | 36.3 | 39.8 | 31.4 |
| Leu Cβ + Cys 2Cβ[h] | 38.9 | 294.6 | 39.1 | 142.7 | e | | e | |
| Tyr Cβ | 37.9 | c | 38.0 | c | f | | f | |
| Ile Cβ | 36.9[i] | | f | | f | | f | |
| Phe Cβ (+Ile Cβ)[g] | 36.5 | c | 36.6 | 67.3 | 36.7 | c | 36.6 | 68.7 |
| Glu Cγ | 33.9 | 28.02 | 34.1 | 28.6 | 33.9 | 91.2 | 34.0 | 38.2 |
| Gln Cγ | 31.4 | 41.3 | 31.6 | 36.7 | 31.4 | c | 31.5 | 72.2 |
| Lys Cβ + Val Cβ + Met Cβ[h] | 30.7 | c | 30.6 | 286.1 | 30.7 | c | 30.9 | 127.7 |
| Pro Cβ + Met Cγ[h] | 29.7 | c | 29.8 | 274.4 | 29.7 | c | 29.8 | 294.8 |
| Val Cβ | 29.3[i] | | e | | e | | e | |
| Arg Cβ + Glu Cβ | 28.0 | 115.5 | 28.2 | 124.1 | 27.9 | c | 28.2 | 114.4 |
| Lys Cβ | 27.1 | 129.6 | 27.1 | 119.5 | 27.2 | c | 26.9 | 114.4 |
| Lys Cδ + Gln Cβ | 26.7 | 129.6 | e | | 26.7 | c | 26.9 | 114.4 |
| Arg Cγ + Ile Cγ1 + Pro Cγ (+ GlcNAc methyl)[g] | 24.8 | 242.4 | 25.0 | 55.4 | 24.7 | c | 25.0 | 42.3 |
| Leu Cγ | 24.4[i] | | e | | 25.0[i] | | e | |
| Lys Cγ | 22.3 | 247.0 | 22.6 | 36.0 | 22.3 | c | 22.6 | 28.8 |
| Leu 2Cδ | 21.1 | c | 21.3 | 130.1 | 21.5[i] | | 21.1 | 35.6 |
| Thr Cγ | 19.2 | c | 19.3 | 92.3 | 19.2[i] | | 19.3 | 79.9 |
| Val Cγ1 | 18.7 | c | 18.9 | 88.8 | 18.8[i] | | 18.9 | 71.0 |
| Val Cγ2 | 18.1 | c | 18.4 | 110.7 | d | | 18.4 | 78.8 |
| Ala Cβ | 17.2[i] | | 17.1 | c | 17.2[i] | | 17.0 | 33.1 |
| Ile Cγ2 + Met Cε[h] | 15.2 | c | 15.2 | 26.5 | f | | 15.2 | 23.8 |
| Ile Cδ | 11.0 | c | 10.7 | 37.0 | d | | 10.7 | 31.3 |

[a] Chemical shifts in parts per million, acetonitrile as reference at 1.300 ppm. [b] Bandwidth at half-height (Hz). [c] Bandwidth calculation unreliable. [d] Merged with preceding peak. [e] Peak intensity too low to permit assignment. [f] Cannot be assigned separately from surrounding peak envelope. [g] β-Conglycinin only. [h] Glycinin only. [i] Peak assigned (Fisher et al., 1990) via the APT pulse sequence (Patt and Shoolery, 1983).

tural information (such as approximate relative degree of structure) is available from the apparent envelope areas. Conversely, the relaxation of nuclei in poorly structured and/or mobile regions in proteins is dominated by spin–

**Table II. Glycinin Peak Assignments, Positions, and Bandwidths at Different Temperatures**

| | 25 °C | | 55 °C | | 70 °C | | 95 °C | | gel | |
|---|---|---|---|---|---|---|---|---|---|---|
| peak assignment | ppm[a] | bw[b] | ppm | bw | ppm | bw | ppm | bw | ppm | bw |
| Glu Cδ | 181.6 | 26.2 | 181.5 | 24.9 | 181.4 | 26.4 | 181.4 | 33.0 | 181.5 | 28.0 |
| Gln Cδ | 178.0 | 38.6 | 178.0 | 45.4 | 178.0 | 48.7 | 178.2 | 55.7 | 178.0 | 36.1 |
| C=O + Asn Cγ | 173.6 | 97.1 | 173.7 | 153.9 | 173.7 | 112.4 | 173.8 | 113.5 | 173.8 | 143.9 |
| C=O | 172.1 | 215.0 | 172.2 | 198.6 | 172.2 | 208.2 | 172.5 | 196.7 | 172.2 | 200.8 |
| Arg Cζ | 157.2 | 20.8 | 157.4 | 20.5 | 157.5 | 21.0 | 157.8 | 19.1 | 157.1 | 19.7 |
| Tyr Cζ | 154.8 | 50.6 | 155.2 | 23.0 | 155.4 | 16.2 | 155.4 | 20.0 | 154.9 | *c* |
| Phe Cγ | 136.5 | *c* | 136.7 | 124.1 | 136.7 | 96.2 | 136.6 | 64.8 | 136.4 | 37.1 |
| His Cγ + $His^+$ Cγ | 135.2 | 40.5 | 135.8 | 40.9 | 136.0 | 84.2 | 136.3 | 89.9 | *e* | |
| His Cε | *e* | | 135.1 | 126.2 | *e* | | *e* | | 134.8 | 50.7 |
| Tyr 2Cδ | 131.1 | 225.5 | 131.1 | 40.9 | 131.1 | 39.2 | 131.1 | 37.7 | 130.8 | 208.6 |
| Phe 2Cδ | 129.5 | 62.4 | 129.7 | 55.8 | 129.7 | 56.9 | 129.8 | 50.1 | 129.5 | 53.9 |
| Phe 2Cε | 129.1 | 68.4 | 129.5 | 64.2 | 129.5 | 56.9 | 129.3 | 54.5 | 129.0 | 57.5 |
| $His^+$ Cε | 128.5 | 227.3 | 128.1 | 212.1 | 128.0 | 201.1 | *e* | | 128.0 | 224.9 |
| Phe Cζ + Tyr Cγ + Trp Cδ2 | 127.5 | 247.4 | 127.5 | 267.1 | 127.6 | 224.4 | 127.7 | 40.0 | 127.5 | 215.9 |
| Trp Cδ1 | 125.5 | *c* | *e* | | 125.6 | *c* | 125.0 | *c* | 124.9 | *c* |
| Trp Cη | 122.3 | 94.4 | 122.3 | 52.3 | 122.6 | 25.3 | 122.2 | 23.5 | *e* | |
| $His^+$ Cδ + Trp Cε3 | 118.9 | 88.0 | 118.9 | 23.9 | 118.9 | 177.4 | 118.7 | 77.5 | *e* | |
| His Cδ + Trp Cζ2 | 117.6 | 40.4 | 117.9 | 82.2 | 118.1 | 49.0 | 118.3 | 76.9 | 117.7 | 53.5 |
| Tyr 2Cε | 115.8 | 39.0 | 116.3 | 41.2 | 116.4 | 38.0 | 116.3 | 31.1 | 115.8 | 31.4 |
| Trp Cζ1 | *e* | | 112.4 | 20.5 | 112.3 | 16.9 | 112.4 | 17.3 | 112.3 | *c* |
| Thr Cβ | 68.2 | 45.9 | 67.4 | 32.9 | 67.5 | 31.8 | 67.7 | 29.0 | 67.4 | 35.8 |
| Ser Cβ | 61.4 | 171.6 | 61.6 | 178.0 | 61.6 | 180.3 | 61.9 | 175.8 | 61.4 | 162.3 |
| *trans*-Pro Cα | 60.9 | *c* | 61.0 | 180.1 | 61.1 | 175.9 | 61.3 | 181.3 | 60.9 | 169.4 |
| Cα Env + *cis*-Pro Cα | 59.6 | *c* | 60.0 | *c* | 60.0 | *c* | 59.4 | 183.6 | 59.7 | 193.2 |
| Cα Env | 57.6 | *c* | 57.3 | *c* | 57.4 | 414.0 | 57.5 | 418.9 | *f* | |
| Ser Cα | 55.9 | *c* | 55.8 | 353.5 | 55.9 | 348.6 | 56.1 | 284.7 | 55.9 | 324.4 |
| Cα Env | 55.0 | 296.6 | 55.1 | 306.1 | 55.2 | 301.3 | 55.4 | 234.1 | *f* | |
| Cα Env | 53.9 | 105.0 | 54.2 | 104.9 | 54.3 | 104.1 | 54.5 | 106.8 | 54.0 | 94.6 |
| Asn Cα | 52.0 | 307.8 | 52.1 | 303.5 | 52.1 | 296.7 | 52.9 | 230.6 | 52.4 | 268.8 |
| Pro Cδ | 48.0 | *c* | 48.3 | 75.6 | 48.3 | 84.4 | 48.5 | 46.2 | 48.2 | 49.2 |
| Gly Cα | 42.9 | *c* | 43.1 | 406.1 | 43.1 | *c* | 43.5 | 32.1 | 42.9 | 46.7 |
| Lys Cε + Arg Cδ | 41.0 | 144.6 | 41.1 | 151.6 | 41.2 | 143.4 | 41.5 | 31.2 | 40.9 | 35.2 |
| Asp Cβ | *f* | | 40.2 | 88.5 | 40.3 | 90.5 | 40.6 | 96.7 | 39.7 | 33.2 |
| Asn Cβ | 39.6 | 40.2 | 39.9 | 87.5 | 39.9 | 87.0 | 40.1 | 96.7 | *f* | |
| Leu Cβ + Cys 2Cβ | 38.9 | 294.6 | 39.3 | 187.2 | 39.4 | 173.0 | 39.4 | 105.0 | 38.7 | 285.7 |
| Tyr Cβ | 37.9 | *c* | *e* | | *e* | | 37.3 | 78.3 | *e* | |
| Ile Cβ | 36.9[g] | *c* | *f* | | *f* | | *f* | | *f* | |
| Phe Cβ | 36.5 | *c* | 36.8 | 304.4 | 36.9 | 329.6 | 36.9 | 72.8 | 36.3 | 292.4 |
| Glu Cγ | 33.9 | 28.0 | 34.0 | 27.8 | 34.1 | 27.7 | 34.4 | 24.5 | 33.8 | 26.9 |
| Gln Cγ | 31.4 | 41.3 | 31.6 | 37.6 | 31.6 | 35.5 | 31.9 | 26.8 | 31.5 | 33.1 |
| Lys Cβ + Val Cβ + Met Cβ | 30.7 | *c* | 30.4 | *c* | 30.4 | *c* | 30.7 | 275.7 | 30.6 | 292.6 |
| Pro Cβ + Met Cγ | 29.7 | *c* | 29.7 | 287.8 | 29.7 | 286.8 | 29.9 | 274.5 | 29.7 | 295.2 |
| Val Cβ | 29.3[g] | *c* | *d* | | *d* | | *d* | | *d* | |
| Arg Cβ + Glu Cβ | 28.0 | 115.5 | 28.3 | 111.2 | 28.3 | 113.4 | 28.7 | 55.6 | 28.0 | 111.6 |
| Lys Cδ | 27.1 | 129.6 | 27.2 | 287.3 | 27.3 | 285.7 | 27.5 | 125.3 | 27.0 | 116.5 |
| Gln Cβ | 26.7 | 129.6 | 26.8 | 289.0 | 26.8 | 292.0 | 27.1 | 273.7 | 26.7 | 116.5 |
| Arg Cγ + Pro Cγ + Ile Cγ1 | 24.8 | 242.4 | 24.9 | 49.8 | 24.9 | 46.1 | 25.1 | 30.3 | 24.8 | 47.2 |
| Leu Cγ | 24.4[g] | | | | | | | | | |
| Lys Cγ | 22.3 | 247.0 | 22.4 | 45.4 | 22.4 | 43.9 | 22.7 | 37.2 | 22.5 | 42.5 |
| Leu 2Cδ | 21.1 | *c* | 21.5 | 408.2 | 21.5 | *c* | 21.8 | 90.8 | 21.1 | 129.0 |
| Thr Cγ | 19.2 | *c* | 19.2 | *c* | 19.0 | *c* | 19.2 | 44.7 | 19.1 | 80.6 |
| Val Cγ1 | 18.7 | *c* | 18.9 | *c* | 18.9 | *c* | 18.4 | 99.1 | 18.8 | 80.6 |
| Val Cγ2 | 18.1 | *c* | 18.3 | *c* | 18.4 | *c* | 18.4 | 114.8 | 18.1 | 102.2 |
| Ala Cβ | 17.2[g] | *c* | 17.1 | *c* | 17.2 | *c* | 17.4 | 39.4 | 17.0 | *c* |
| Ile Cγ2 + Met Cε | 15.2 | 458.2 | 15.3 | 37.1 | 15.3 | 41.2 | 15.6 | 27.2 | 15.1 | 26.6 |
| Ile Cδ | 11.0 | *c* | 10.6 | 29.6 | 10.6 | 38.2 | 10.9 | 32.3 | 10.5 | 36.6 |

[a] Chemical shifts in parts per million, acetonitrile as reference at 1.300 ppm. [b] Bandwidth at half height (Hz). [c] Bandwidth calculation unreliable. [d] Merged with preceding peak. [e] Peak intensity too low to permit assignment. [f] Cannot be assigned separately from surrounding peak envelope. [g] Peak assigned (Fisher et al., 1990) via the APT plus sequence (Patt and Shoolery, 1983).

lattice interactions. This plus an accompanying increased nuclear Overhauser enhancement (NOE) results in a peak that is both narrower and more intense in the unstructured and mobile regions of a protein than the peak for the same carbon in nonrandom or structured regions (Levy et al., 1980; Jardetzky and Roberts, 1981; Wüthrich, 1976) and therefore relatively easy to assign. Such peaks provide information on the differences and similarities in microstructure and composition between glycinin and β-conglycinin, but only limited amounts of conformational information. Unfortunately, the interdependence of frequency, correlation time, bandwidth, spin–lattice relaxation time ($T_1$), and spin–spin relaxation time ($T_2$) limits the usefulness of carbon relaxation measurements when applied to protein dynamics.

In the presence of a strong denaturant such as 6 M urea, two phenomena occur: First, there is a thorough unfolding of the secondary structure of soy storage proteins to a poorly ordered conformation (Lillford, 1978), decreasing the number of dissimilar internal environments versus that observed in the native protein. Second, the proteins dissociate into subunits, glycinin into six disulfide-linked acidic–basic polypeptide pairs and β-conglycinin into three monomeric subunits (Nielsen, 1985). These changes produce a large increase in local motion of both the protein backbone and amino acid side chains

**Table III. β-Conglycinin Peak Assignments, Positions, and Bandwidths at Different Temperatures**

| peak assignment | 25 °C | | 55 °C | | 70 °C | | 85 °C | | gel | |
|---|---|---|---|---|---|---|---|---|---|---|
| | ppm[a] | bw[b] | ppm | bw | ppm | bw | ppm | bw | ppm | bw |
| Glu Cδ | 181.5 | 363.1 | 181.4 | c | 181.3 | 160.1 | 181.3 | 91.0 | 181.6 | 380.6 |
| Gln Cδ | 178.0 | c | 178.1 | 418.4 | 178.1 | 439.5 | 178.2 | 63.8 | 178.1 | 391.4 |
| C=O + Asn Cγ | 174.0 | 89.0 | 174.0 | 141.3 | 174.0 | 148.6 | 174.0 | 115.7 | 174.0 | 82.7 |
| C=O | 172.4 | 221.2 | 172.2 | 208.9 | 172.1 | 211.4 | 172.0 | 210.2 | 172.4 | 240.9 |
| C=O | 172.0 | 220.8 | d | | d | | d | | 172.0 | 240.9 |
| Arg Cζ | 157.1 | 22.9 | 157.4 | 20.7 | 157.5 | 21.5 | 157.6 | 28.0 | 157.1 | 21.7 |
| Phe Cγ | 136.5 | 34.4 | 136.6 | 128.5 | 136.5 | 83.4 | 137.0 | 60.8 | 136.5 | 68.9 |
| His Cγ + Cε + $His^+$ Cγ | 135.6 | c | 135.7 | 131.1 | 135.8 | 172.2 | 135.6 | 127.6 | 135.0 | 38.5 |
| Tyr 2Cδ | 131.1 | 257.9 | f | | 130.9 | 291.0 | 130.8 | 225.8 | 130.8 | 219.8 |
| Phe 2Cδ + $His^+$ Cε | 129.6 | 111.6 | 129.7 | 129.8 | 129.6 | 142.0 | 129.6 | 68.3 | 129.6 | 84.0 |
| Phe 2Cε | 129.0 | 113.0 | 129.2 | 130.3 | 129.1 | 138.6 | 129.2 | 65.0 | 129.0 | 112.9 |
| Phe Cζ + Tyr Cγ | 127.3 | 245.7 | 127.5 | 237.0 | 127.6 | 257.3 | 127.6 | 222.6 | 127.4 | 291.2 |
| $His^+$ Cδ | d | | d | | 120.1 | 24.4 | 120.2 | 35.5 | d | |
| His Cδ | 118.3 | 69.7 | 118.6 | 34.6 | 118.6 | 107.0 | 118.4 | 62.8 | f | |
| Tyr 2Cε | 115.8 | 23.0 | 116.0 | 40.5 | 116.1 | 55.6 | 116.3 | 30.6 | 115.87 | 22.7 |
| α-Man C1 | 102.6 | 26.0 | 102.6 | 17.2 | 102.5 | 23.5 | 102.7 | 27.4 | 102.5 | 17.1 |
| GlcNAc(Asn) C1 | 101.2 | 44.1 | 101.1 | 13.9 | 101.1 | 23.8 | d | | | |
| GlcNAc(Asn) C2 | 78.7 | 50.4 | 78.9 | 39.3 | 78.8 | 27.4 | 78.9 | 54.2 | d | |
| α-Man C5 | 73.5 | c | 73.7 | 51.3 | 73.9 | 42.4 | 73.7 | c | 73.5 | 41.7 |
| α-Man C2, C3, C4 | 70.5 | 94.2 | 70.5 | 52.4 | 70.7 | 45.7 | 70.8 | 86.7 | 70.7 | 60.2 |
| Thr Cβ + β-Man C4, C6 | 67.2 | c | 67.4 | 41.9 | 67.5 | 34.9 | 67.6 | 123.8 | 67.3 | 39.9 |
| Ser Cβ + α-Man C6 | 61.5 | 99.5 | 61.6 | 70.3 | 61.6 | 82.5 | 61.8 | 74.7 | 61.4 | 96.4 |
| Pro Cα + GlcNAc(Asn) C2 | 60.7 | 383.4 | 60.9 | 118.6 | 60.9 | 144.7 | 61.1 | 132.6 | 60.7 | 102.9 |
| Cα Env (+GlcNAc(α-Man) C2) | 56.2 | 118.1 | 55.8 | c | 56.1 | 347.4 | 56.1 | 316.1 | 56.1 | 365.1 |
| Ser Cα | 55.9 | c | f | | f | | f | | f | |
| Cα Env | 54.1 | 85.3 | 54.2 | 79.4 | 54.4 | 74.9 | 54.5 | 73.3 | 54.1 | 73.3 |
| Asn Cα | 52.1 | c | 52.3 | 404.7 | 52.4 | 349.2 | 51.6 | c | 52.1 | 336.0 |
| Pro Cδ | 48.3 | c | 48.3 | c | 48.3 | c | 48.4 | 66.0 | 48.3 | 47.3 |
| Gly Cα | 42.9 | c | 43.1 | c | 43.2 | c | 43.3 | c | 42.9 | c |
| Lys Cε + Arg Cδ | 41.0 | 115.4 | 41.1 | 39.7 | 41.2 | 33.1 | 41.3 | 32.2 | 40.9 | 30.4 |
| Asp Cβ + Asn Cβ + Leu Cβ | 39.7 | 36.3 | 39.9 | 33.9 | 40.0 | 32.8 | 40.0 | 46.3 | 39.7 | 29.2 |
| Phe Cβ + Ile Cβ | 36.7 | c | 36.6 | c | 36.8 | c | 36.8 | 317.6 | 36.2 | |
| Glu Cγ | 33.9 | 91.2 | 34.0 | 57.1 | 34.1 | 35.5 | 34.2 | 29.9 | 33.9 | 91.2 |
| Gln Cγ | 31.4 | c | 31.6 | c | 31.6 | 91.3 | 31.7 | 92.5 | 31.4 | 126.0 |
| Lys Cβ + Val Cβ | 30.7 | c | 30.8 | c | 30.8 | c | 30.9 | 297.8 | 30.7 | 299.5 |
| Pro Cβ | 29.7 | c | 29.7 | c | 29.7 | c | 29.7 | 308.8 | 29.7 | 307.2 |
| Arg Cβ + Glu Cβ | 27.9 | 116.8 | 28.4 | 50.2 | 28.3 | 111.2 | 28.0 | 123.8 | 28.0 | 107.5 |
| Lys Cβ | 27.2 | c | f | | f | | 27.4 | 287.5 | 27.2 | 133.1 |
| Lys Cδ + Gln Cβ | 26.7 | 135.0 | 26.6 | 133.3 | 26.8 | 133.6 | 26.8 | 177.9 | 26.6 | 121.2 |
| Arg Cγ + Leu Cγ + Pro Cγ + Ile Cγ1 + GlcNAc methyl | 25.0 | c | 24.9 | 72.8 | 24.9 | 53.6 | 25.0 | 37.3 | 24.9 | 60.5 |
| Lys Cγ | 22.3 | c | 22.4 | c | 22.4 | 508.0 | 22.5 | 44.3 | 22.3 | 35.3 |
| Leu 2Cδ | 21.5[g] | c | f | | 21.4 | c | 21.6 | c | 21.2 | c |
| Thr Cγ | 19.2[g] | c | 19.3 | c | 19.3 | c | 19.0 | 92.4 | 18.8 | c |
| Val Cγ | 18.8[g] | 18.9 | f | | 18.9 | c | 18.4 | 91.5 | 18.2 | c |
| Ala Cβ | 17.2[g] | c | 17.1 | c | 17.3 | c | 17.3 | 48.4 | 17.0 | c |
| Ile $Cγ_2$ | 15.6[g] | c | 15.6 | c | 15.7 | c | 15.5 | 39.0 | 15.1 | c |
| Ile Cδ | 10.7[g] | c | 10.8 | 36.2 | 10.7 | c | 10.7 | 56.8 | 10.5 | 31.0 |

[a] Chemical shifts in parts per million, acetonitrile as reference at 1.300 ppm. [b] Bandwidth at half-height (Hz). [c] Bandwidth calculation unreliable. [d] Merged with preceding peak. [e] Peak intensity too low to permit assignment. [f] Cannot be assigned separately from surrounding peak envelope. [g] Peak assigned (Fisher et al., 1990) via the APT pulse sequence (Patt and Shoolery, 1983).

and a decrease in correlation time ($\tau_C$), resulting in an increase in $T_1$, a larger increase in $T_2$, and, therefore, a decrease in the $T_1/T_2$ ratio. The observable results are narrower peaks, smaller peak envelopes, an increase in signal intensity and peak definition, and a spectrum that more closely resembles that of mixture of free amino acids than does the native protein. These changes can be seen in Figure 1 and Table I, which summarize chemical shift and bandwidth data for glycinin and β-conglycinin prior to and after denaturation with 6 M urea.

The presence of urea had the anticipated effect on the $^{13}C$ NMR spectrum of glycinin as seen in Table I and Figure 1A,B. Several peaks were observed (Figure 1B) that had previously been unobservable due to their broadness and/or presence under a peak envelope (Figure 1A). Several such "new" peaks appeared in the aliphatic region (10–50 ppm) and in the 50–65 ppm region, which includes resonances from the peptide backbone carbons (α-carbons). This is emphasized by the appearance in denatured glycinin of the peak at 17.2 ppm, assigned to the β-carbon of alanine. This peak appears in native glycinin (Figure 1A) as a shoulder that could only be accurately observed and assigned with the APT sequence (Fisher et al., 1990). After denaturation with 6 M urea (Figure 1B), it can be clearly observed, although the bandwidth cannot be reliably calculated (Table I).

On denaturation, the aromatic regions (115–140 ppm) of both glycinin and β-conglycinin spectra, associated with carbons of phenylalanine, tyrosine, and histidine, show similar changes from those of the native materials (see Figure 1). In both spectra, the peaks around 130 ppm, assigned to phenylalanine, become taller and narrower relative to the remainder of the peaks in the spectrum. This suggests that Phe is far more mobile in the denatured proteins. This phenomenon was also observed by Dev et al. (1988) using FT-IR. A similar effect is seen in the appearance of the Tyr Cζ peak at 155 ppm in denatured β-conglycinin and various tryptophan peaks (112, 118, 119, 122 ppm) in glycinin.

The concentration of tryptophan in glycinin is too low for more than a few protonated carbons in it to be assigned under the experimental conditions used herein. Also

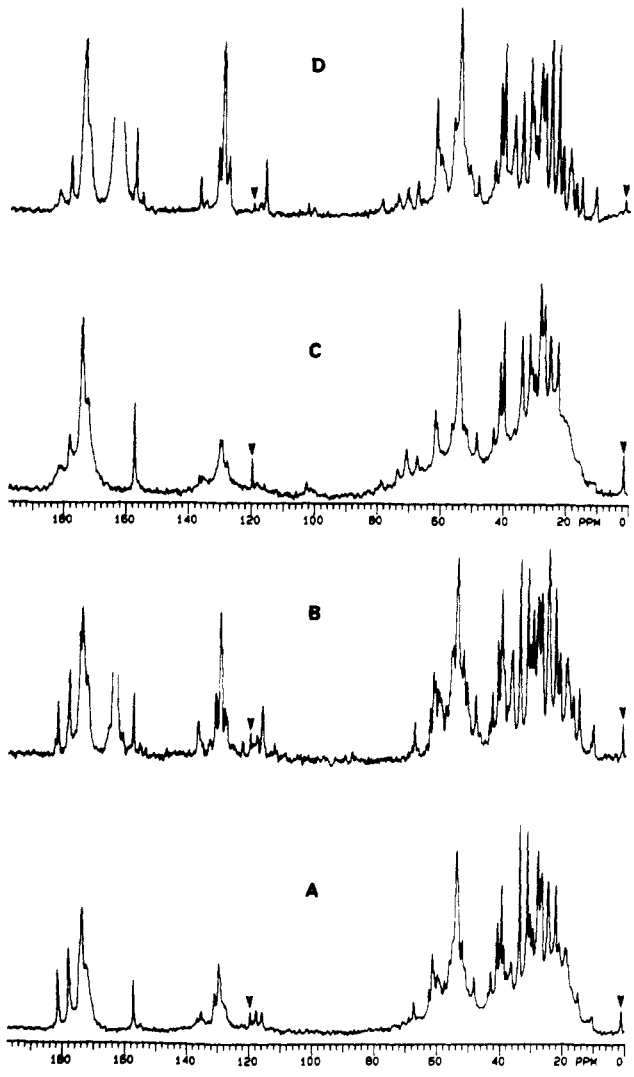


**Figure 1.** Carbon-13 NMR spectrum at 25 °C: (A) glycinin in pH 7.0, 0.035 M phosphate buffer containing 0.4 M NaCl, 192 000 transients; (B) glycinin denatured in 6.0 M urea, pH 7.0, containing 0.035 M phosphate buffer and 0.4 M NaCl, 48 000 transients; (C) β-conglycinin in pH 7.0, 0.035 M phosphate buffer containing 0.4 M NaCl, 144 000 transients; (D) β-conglycinin denatured in 6.0 M urea, pH 7.0, containing 0.035 M phosphate and 0.4 M NaCl, 48 000 transients. Large peaks in B and D at 160 ppm are urea. Arrows at 1.3 and 119.6 ppm denote peaks from the acetonitrile internal reference.

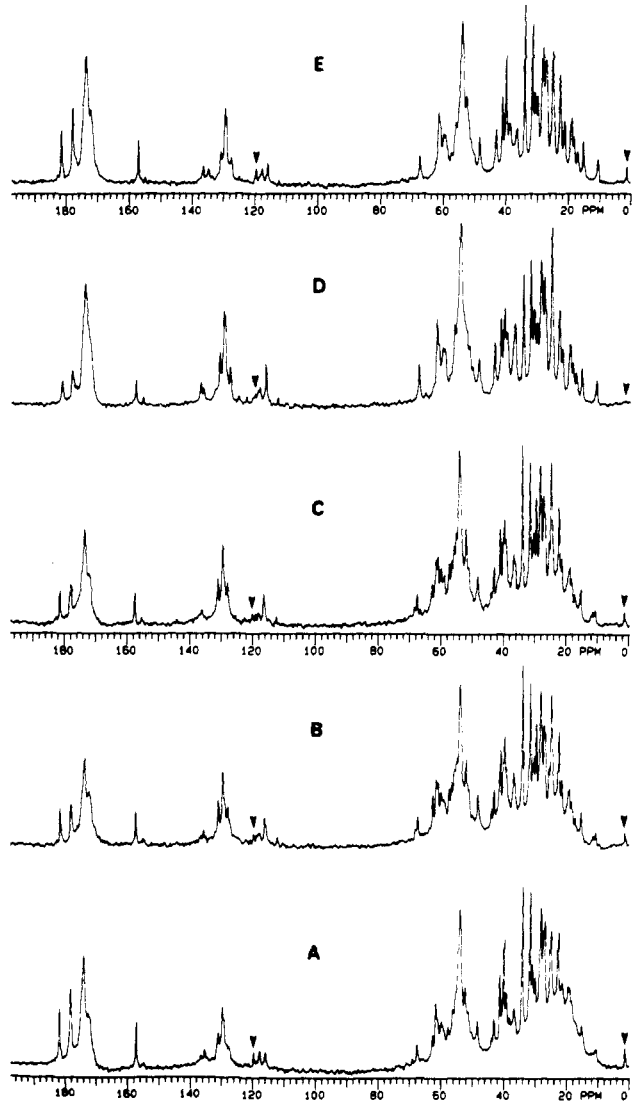


**Figure 2.** Carbon-13 NMR spectra in pH 7.0, 0.035 M phosphate buffer containing 0.4 M NaCl: (A) glycinin at 25 °C, 192 000 transients; (B) 70 °C; (C) 85 °C; (D) 95 °C (pregel aggregate); (E) glycinin gel at 25 °C. Spectra B–E acquired with 144 000 transients. Arrows at 1.3 and 119.6 ppm denote peaks from the acetonitrile internal standard.

because of low concentrations, methionine and cysteine/cystine peaks could not be identified as distinct peaks, though they contribute to bands containing other carbons (Table I). A small number of new peaks were seen in the carbonyl region (165–185 ppm).

Of note in this region is the appearance of a second peak in area assigned to the glutamate side-chain carboxyl (182 ppm). This new peak can be explained by changes in the involvement of glutamate interactions in the denatured protein, e.g., hydrophilic interactions with hydroxylated side chains or electrostatic interactions with positively charged side chains. Many of the existing glycinin peaks (Figure 1A) became sharper (Figure 1B) and narrower (Table I) due to decreased $T_1/T_2$ ratios upon denaturation.

Urea had a similar, though much more pronounced, effect on the β-conglycinin spectrum (compare parts C and D of Figure 1). The region most affected by chemical denaturation of β-conglycinin was the aliphatic hydrocarbon region (10–45 ppm), which contains the methyl ($CH_3$) and methylene ($CH_2$) groups arising primarily from valine, leucine, isoleucine, alanine, and proline. These functional groups readily form stable hydrophobic interactions in the interior of proteins through the exclusion of water, restricting their mobility and resulting in $T_2$-broadened, overlapping peaks that form large envelopes (Fisher et al., 1990) in native β-conglycinin (Figure 1C). In the denatured protein (Figure 1D), these interactions are disrupted, producing the effect described above. This effect can also be seen between 60 and 80 ppm, where the apparent extension of the α-carbon peak envelope in Figure 1C collapses almost to base line in Figure 1D. The peaks in this region are from hydroxyl-containing amino acid side chains (Ser $C^{\alpha}$ near 61 ppm, Thr $C^{\beta}$ near 67 ppm) and the carbohydrate moiety (Table I). These changes in the carbohydrate ring carbon peaks (61–80 ppm) strongly suggest the involvement of the carbohydrate moiety in β-conglycinin's native secondary structure, supporting observations made on the native proteins themselves (Fisher et al., 1990).

Very few new peaks were observed in the other regions of the β-conglycinin spectrum (compare parts C and D of Figures 1), although many existing peaks became narrower (Table I) and more intense (Figure 1D). This is

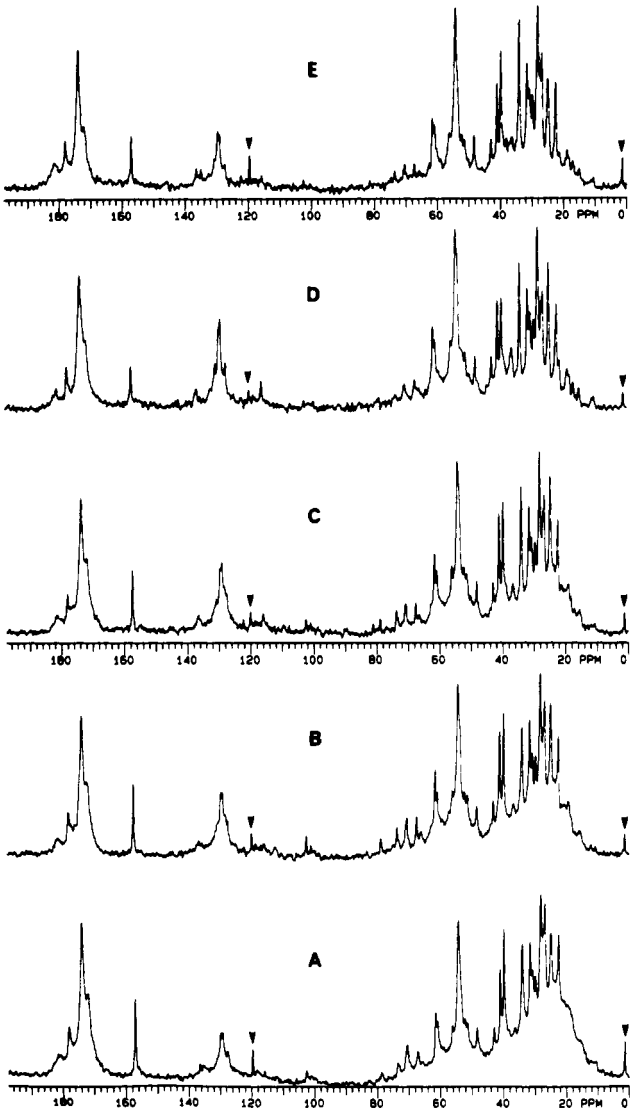


**Figure 3.** Carbon-13 NMR spectra in pH 7.0, 0.035 M phosphate buffer containing 0.4 M NaCl: (A) β-conglycinin at 25 °C, 192 000 transients; (B) 55 °C; (C) 70 °C; (D) 85 °C (pregel aggregate); (E) β-conglycinin gel at 25 °C. Spectra B–E acquired with 144 000 transients. Arrows at 1.3 and 119.6 ppm denote peaks from the acetonitrile internal standard.

particularly noticeable for the β-conglycinin tyrosine Cζ at 155 ppm (Figure 1D), which cannot be observed in the native (Figure 1C) protein.

The glutamate side-chain carboxyl peak at 182 ppm is of note in that even in the denatured protein it remains broad. This implies that the interactions involving the glutamate carboxyl are strong enough to survive the perturbations of chemical denaturation. The differences in the native and denatured spectra of both glycinin and β-conglycinin make it likely that glutamate is involved in β-conglycinin structure and unlikely that it is involved in glycinin structure.

Major differences between the apparent sizes of the peak envelopes in the spectra of both native and urea-denatured glycinin and β-conglycinin were seen (Figure 1). Denaturation of glycinin produced a comparatively small reduction in the size of the peak envelopes (Figure 1A,B), primarily in the aliphatic region (10–45 ppm). By contrast, denaturation of β-conglycinin caused a large reduction in envelope size in every region of the spectrum (Figure 1C,D). These differences can also be seen in bandwidth changes (Table I). Disruption of hydrogen bonds and hydrophobic interactions by urea had some effect on glycinin denaturation, but the presence of an observable peak envelope implies partial retention of structure. A significant role in partial retention of structure by glycinin must be played by disulfide bonds, which are unaffected by urea (Nielsen, 1985). The disulfide bonds in glycinin cause regions of each pair of polypeptide chains to remain in close proximity, even on chemical denaturation, allowing interchain interactions that can be observed as an aliphatic peak envelope that is larger in denatured glycinin than in the equivalent region of the β-conglycinin spectrum (compare parts B and D of Figure 1). The retention of structure can also be seen in Table I as bandwidths that in many cases decreased only slightly (e.g., Gln Cγ, 31.4 ppm; and Lys Cβ, 27.1 ppm) and in some cases increased (e.g., Glu Cγ, 33.9 ppm; and Arg Cβ/Glu Cβ, 28 ppm) on denaturation. There is little or no cysteine found in β-conglycinin (Coates et al., 1985) and no disulfide bonds (Thanh and Shibasaki, 1977). Thus, it should be more susceptible to urea denaturation than should glycinin. That is clearly the case from our results (Figure 1). The amino acid residues contributing the most to β-conglycinin conformation appear to come from the aliphatic (10–45 ppm) and aromatic (115–140 ppm) regions, though the carbohydrate peak envelope (65–80 ppm) also decreases in area, implying involvement of that moiety in β-conglycinin structure as well. It should also be noted that, for both proteins, the amino acid and (in β-conglycinin) carbohydrate chemical shifts (60–105 ppm) changed very little when the proteins were chemically denatured, confirming that the sharp peaks observed in the native proteins were largely from mobile groups in random regions.

**Influence of Heating.** When glycinin and β-conglycinin were heated above room temperature, chemical shift, bandwidth, and line shape of the dominant peaks changed only slightly with increasing temperature (Tables II and III; Figures 2B,C and 3B,C), supporting the occurrence in both native proteins of large unstructured regions (Ishino and Kudo, 1980) that are not greatly affected by temperatures at or below the gelation point (Suresh Chandra et al., 1984). In both proteins, the dominant peaks in the aliphatic and aromatic regions, which belong to amino acids with charged side groups, have bandwidths in the native proteins at 25 °C that are very similar to those in the heat-treated, partially unfolded proteins (Tables II and III). Thus, the amino acids associated with the dominant peaks are not greatly motion-constrained, consistent with these amino acid side chains being located on the exterior of the protein.

In both glycinin and β-conglycinin, aliphatic and aromatic interactions appear to be important to the maintenance of structure. Thus, the changes in peak shape and definition during heating are directly related to structural changes. Peaks in the aliphatic (10–45 ppm) and aromatic (115–140 ppm) regions became sharper, and fine structure emerged in the 10–20 ppm envelope of the β-conglycinin spectrum (Figures 2 and 3) as the temperature was increased. The aliphatic and α-carbon envelopes in both protein spectra (Figures 2A and 3A) decreased in area with increasing temperature, particularly at 95 °C for glycinin (Figure 2D) and 85 °C for β-conglycinin (Figure 3D). This indicates that the aliphatic side chains and α-carbons are less dominated by $T_2$ line broadening (Levy et al., 1980; Jardetzky and Roberts, 1981; Wüthrich, 1976).

The probable cause of these spectral changes is 2-fold. At the lowest temperatures above 25 °C, the polypeptide chains unfold. At higher temperatures, the partly

unfolded proteins undergo intersubunit and/or intermolecular interactions to form soluble aggregates (Hermansson, 1986; Mori et al., 1986; Nakamura et al., 1986a,b). Glycinin, when heated to 95 °C, and β-conglycinin heated to 85 °C are referred to as being in a pregel state, characterized (Hermansson, 1986; Mori et al., 1986; Nakamura et al., 1986a,b) by the conversion of the protein aggregates formed at temperatures below the gelation temperature to interconnected strands.

These stages are particularly easy to see in β-conglycinin. At room temperature (Figure 3A), the β-conglycinin methyl peaks (10–21 ppm) appear as blunt shoulders on the aliphatic peak envelope (10–80 ppm). At 55 °C (Figure 3B), these shoulders become flat-topped "shelves" that persist at 70 °C (Figure 3C). At 85 °C, the β-conglycinin gelation temperature, these shelves have separated into distinct peaks. A parallel change in the aromatic peaks can also be seen. At the same time, the carbohydrate peaks around 70 ppm have gone from being distinct at 55 and 70 °C to being broad and ill-defined at 85 °C.

Equivalent changes in spectral characteristics occur in glycinin as well, but are much less obvious. As with β-conglycinin, the glycinin methyl region undergoes a marked change when heated from 25 °C (Figure 2A) to 55 °C (Figure 2B). Little or no change occurs on heating to 70 °C (Figure 3C). At 95 °C (Figure 2D), methyl peak definition increases, the peaks around 130 ppm become sharper, and those around 60 ppm become fewer.

The spectra of chemically (Figure 1B,D) and heat-denatured glycinin (Figure 2D) and β-conglycinin (Figure 3D) differ markedly from one another. In particular, the degree of denaturation, apparent in the number of transients required to obtain equivalent signal to noise ratios (see captions to Figures 1–3), is far larger when 6 M urea is used than when the proteins are heated to their gelation temperatures. This strongly suggests, as FT-IR results did to Dev et al. (1988), that the configurational changes during chemical and heat denaturation are very different and probably result from the retention of interactions during the change from native protein to aggregate to strand to gel during heating that are eliminated by chemical denaturation.

**Influence of Gel Formation.** Glycinin heated to 95 °C and β-conglycinin heated to 85 °C gave firm gels on cooling to 4 °C. Protein samples heated to lower temperatures did not form gels on cooling. On gelation, both proteins give spectra that more closely resemble the spectra obtained at temperatures above 25 °C than those obtained for either the native or chemically denatured proteins. Only one possibility can account for these differences: intermolecular structure having intramolecular regions that are highly random and/or mobile. Structural regularity has been observed in β-conglycinin gels and glycinin aggregates and gels at room temperature by electron microscopy (Hermansson, 1985, 1986; Mori et al., 1986), though the nature of the technique precludes observations at elevated temperatures. The work of these investigators and others (Nakamura et al., 1986a,b; Utsumi and Kinsella, 1985), and the sharp differences between the spectra of chemically denatured (Figure 1B,D) and pregel state (Figures 2D and 3D) and gel state (Figures 2E and 3E) glycinin and β-conglycinin support this conclusion. In the pregel state (Figures 2D and 3D), the spectra of both glycinin and β-conglycinin show peaks throughout the aliphatic and aromatic regions that are more intense and have narrower bandwidths than in spectra obtained either before (Figures 2A–C and 3A–C) or after gelation (Figures 2E and 3E). These peaks decreased in intensity and increased slightly in line width upon gel formation (Figures 2E and 3E), indicating a loss of mobility (but not necessarily randomness) accompanied by shortening of $T_1$ and loss of NOE (Levy et al., 1980; Jardetzky and Roberts, 1981; Wüthrich, 1976).

As in formation of the pregel state, this is most obvious for the methyl (10–21 ppm) peaks in both glycinin and β-conglycinin (Figures 2D,E and 3D,E) and slightly less obvious in the aromatic region around 130 ppm. Structural changes are also indicated by changes in the carbohydrate region of β-conglycinin (around 70 ppm) and around 60 ppm in glycinin. These changes result from an increased intermolecular structural order upon cooling, involving aliphatic and aromatic side chains, evidenced by the decrease in intensity and increase in line width of the aromatic and aliphatic side-chain peaks and by the increase in the size of the aliphatic peak envelopes. These observations, plus those on urea-denatured glycinin and β-conglycinin, indicate that, at the gelation temperatures of glycinin and β-conglycinin, loss of native secondary and tertiary structure by both proteins is only partial. On gelation, both proteins increase in their degrees of structure but, judging from the behavior of the methyl peaks, do not recover native structure. The differences in methyl and aromatic regions between glycinin and β-conglycinin gels indicate that the methyl and aromatic groups in the glycinin gel are more mobile than those in the β-conglycinin gel, strongly implying that the β-conglycinin gel structure is more dense than that of glycinin.

Aggregation and gel formation effects can also be seen in the behavior of the guanidino carbon of arginine peak at 157 ppm in both glycinin and β-conglycinin during heating and cooling. This carbon has no attached protons to provide NOE or $T_1$ dipole–dipole effects and is unaffected by $T_2$ line broadening. It therefore acts very much like a free amino acid and is relatively insensitive to conformational changes. At temperatures above 25 °C in both proteins (Figures 2 and 3), the peak decreased in both intensity and line width, consistent with an increase in $T_1$ resulting from increased freedom of movement in the side chain and with increased intensity of other peaks resulting from the effects of protein unfolding. Upon gelation (Figures 2E and 3E), the peak broadens and increases in intensity. This results from loss of mobility of the side chain itself and loss of peak intensity elsewhere in the spectrum, both due to formation of interstrand structures. Similar effects can be seen (Figures 2D,E and 3D,E) in the peaks resulting from the carboxyl groups of glutamate (182 ppm) and the carboxamide group of glutamine (178 ppm).

Unlike the aliphatic and aromatic peaks in β-conglycinin, the peaks in the carbohydrate region (60–110 ppm) broaden upon formation of the pregel (compare parts C and D of Figure 3) and then exhibit an increase in envelope size upon formation of the gel (Figure 3E). This suggests that, at temperatures below that of the pregel state (Figure 3B,C), these groups are in larger numbers of moderately mobile regions, whereas in both the pregel and gel these regions become more structured, with some regions sufficiently random and/or mobile to provide small, sharp peaks, much as is observed for the chemically denatured protein (Figure 1D). The most probable structural processes for the carbohydrate chain in the gel are intermolecular interactions involved in pregel strand and gel structure formation, most likely interactions with glutamate and other carbohydrate sidechains. This is

supported by the shape of the β-conglycinin glutamate carboxyl at 182 ppm. At all temperatures, it remains a small, broad peak (Table III), consistent with restricted motion, probably due to involvement in intra- and/or interchain bonding. As pointed out for the urea-denatured protein, the fact that the peak shows little or no change in shape or line width during pregel or gel formation signifies its importance in stabilizing some regions of β-conglycinin structure in the face of external perturbations to the protein.

The spectra in Figures 2 and 3 support the theory (Hermansson, 1986; Mori et al., 1986; Nakamura et al., 1986a,b) of a three-step process in soy protein gelation and augment previous information by supplying direct observations of glycinin and β-conglycinin at specific temperatures. Both proteins undergo partial unfolding between 25 and 55 °C. Small changes around 60 and 130 ppm suggest that glycinin aggregation begins at 70 °C and that these aggregates interact to form strands at 95 °C. In β-conglycinin, partial unfolding persists through 70 °C and both aggregates and strands form at 85 °C. Gel formation in both proteins is accompanied by increased restrictions on motion consistent with the coalescence of strands into the gel network. The changes in the methyl region of β-conglycinin imply that its gel is more dense than that of glycinin. In addition, our results support the involvement of the carbohydrate and glutamate side chains in β-conglycinin structure and gel formation.

## SUMMARY

From the data obtained from carbon-13 NMR spectra of glycinin and β-conglycinin under conditions of gelation and heat and chemical denaturation, we conclude that much of their native structure depends on aliphatic and aromatic interactions. Hydrophilic interactions involving carbohydrate and glutamate are important to β-conglycinin secondary structure. These interactions are diminished upon heat and chemical denaturation but reappear upon gelation, indicating that these interactions are important in formation of glycinin and β-conglycinin gels. Furthermore, from the large number of sharp peaks in all the spectra we conclude that *both* of the proteins in *both* native and gelled states have large amounts of relatively mobile structure—random coil and/or flexible β-sheet—consistent with other studies (Dev et al., 1988; Ishino and Kudo, 1980).

The involvement of covalent forces in maintaining gel structure in glycinin and glycinin gels cannot be directly studied by NMR due to the low cysteine content of glycinin. However, the spectra of chemically denatured glycinin lead us to conclude that covalent forces, such as disulfide bonds, also help maintain glycinin structure in part by keeping sections of the acidic and basic polypeptides in close proximity regardless of external perturbations.

## ACKNOWLEDGMENT

We express our gratitude to Dr. Walter J. Wolf, Northern Regional Research Center, USDA—ARS, for supplying purified β-conglycinin. We also thank Drs. Charles A. Kingsbury, University of Nebraska—Lincoln, and William R. Croasmun, Kraft, Inc., for their critical evaluation of this paper. Presented in part at the 196th National Meeting of the American Chemical Society, Los Angeles, CA, Sept 1988.

## LITERATURE CITED

Baianu, I. C. High-Resolution NMR Studies of Food Proteins. In *NMR in Agriculture*; Pfeffer, P., Gerasimowicz, W., Eds.; CRC Press: Cleveland, OH, 1989.

Baianu, I. C.; Johnson, L. F.; Waddell, D. K. High-Resolution Proton, Carbon-13 and Nitrogen-15 Nuclear Magnetic Resonance Studies of Wheat Proteins at High Magnetic Fields: Spectral Assignments. Changes with Concentration and Heating Treatments of Flinor Gliadins in Solution-Comparison with Gluten Spectra. *J. Sci. Food Agric.* **1982**, *33*, 373–83.

Belton, P. S.; Duce, S. L.; Tatham, A. S. $^{13}C$ solution state and solid state n.m.r. of wheat gluten. *J. Biol. Macromol.* **1987**, *9*, 357–63.

Coates, J. B.; Medeiros, J. S.; Thanh, V. H.; Nielsen, N. C. Characterization of Subunits of β-Conglycinin. *Arch. Biochem. Biophys.* **1985**, *243* (1), 184–94.

Dev, S. B.; Keller, J. T.; Rha, C. K. Secondary structure of 11 S globulin in aqueous solution investigated by FT-IR derivative spectroscopy. *Biochim. Biophys. Acta* **1988**, *957*, 272–80.

Fisher, M. S.; Marshall, W. E.; Marshall, H. F., Jr. Carbon-13 NMR Studies of Glycinin and β-Conglycinin at Neutral pH. *J. Agric. Food Chem.*, **1990**, preceding paper in this issue.

Hermansson, A.-M. Physico-chemical aspects of soy protein structures formation. *J. Texture Stud.* **1978**, *9*, 33–58.

Hermansson, A.-M. Structure of Soya Glycinin and Conglycinin Gels. *J. Sci. Food Agric.* **1985**, *36*, 822–32.

Hermansson, A.-M. Soy Protein Gelation. *JAOCS, J. Am. Oil Chem. Soc.* **1986**, *63* (5), 658–66.

Howarth, O. W.; Lilley, D. M. J. Carbon-13 NMR of Peptides and Proteins. *Prog. Nucl. Magn. Reson. Spectrosc.* **1978**, *12*, 1–40.

Ishino, K.; Kudo, S. Conformational Transition of Alkali-Denatured Soybean 7S and 11S Globulins by Ethanol. *Agric. Biol. Chem.* **1980**, *44* (3), 537–43.

Jardetzky, O.; Roberts, G. C. K. Protein Dynamics. In *NMR in Molecular Biology*; Jardetzky, O., Roberts, G. C. K., Eds.; Academic Press: New York, 1981.

Kakalis, L. T.; Baianu, I. C. Carbon-13 NMR study of soy protein conformations in solution. *Fed. Proc.* **1985**, *44*, Abstract 8155.

Kakalis, L.; Baianu, I. C. High resolution carbon-13 NMR studies of soy protein isolates. In High-Resolution NMR Studies of Food Proteins. In *NMR in Agriculture*; Pfeffer, P., Gerasimowicz, W., Eds.; CRC Press: Cleveland, OH, 1989.

Koshiyama, I. Storage Proteins of Soybean. *Cereal Chem.* **1968**, *45*, 394.

Koshiyama, I.; Hamano, M.; Fukushima, D. A Heat Denaturation study of the 11S Globulin in Soybean Seeds. *Food Chem.* **1981**, *6*, 309–22.

Laemmli, U. K. Cleavage of Structural Proteins during the Assembly of the Head of Bacteriophage T4. *Nature (London)* **1970**, *227*, 680.

Levy, G. C.; Lichter, R. L.; Nelson, G. L. Relaxation Studies. *Carbon-13 Nuclear Magnetic Resonance Spectroscopy*, 2nd ed.; Wiley: New York, Chichester, Brisbane, Toronto, Singapore, 1980.

Lillford, P. G. Conformation of Plant Proteins. In *Plant Proteins*; Norton, G., Ed.; Butterworths: London, 1978.

Mori, T.; Nakamura, T.; Utsumi, S. Behavior of Intermolecular Bond Formation in the Late Stage of Heat-induced Gelation of Glycinin. *J. Agric. Food Chem.* **1986**, *34*, 33–6.

Nakamura, T.; Utsumi, S.; Mori, T. Mechanism of Heat-induced Gelation and Gel Properties of Soybean 7S Globulin. *Agric. Biol. Chem.* **1986a**, *50* (5), 1287–93.

Nakamura, T.; Utsumi, S.; Mori, T. Interactions During Heat-induced Gelation in a Mixed System of Soybean 7S and 11S Globulins. *Agric. Biol. Chem.* **1986b**, *50* (10), 2429–35.

Nielsen, N. C. Structure of Soy Proteins. *New Protein Foods* **1985**, *5*, 27–64.

Patt, S. L.; Shoolery, J. N. Attached proton test for carbon-13 NMR. *J. Magn. Reson.* **1982**, *46*, 435.

Shaka, A. J.; Keeler, J.; Frenkiel, T.; Freeman, R. An improved sequence for broadband decoupling: WALTZ-16. *J. Magn. Reson.* **1983**, *52*, 335–8.

Suresh Chandra, B. R.; Appu Rao, A. G.; Narasinga Rao, M. S. Effect of Temperature on the Conformation of Soybean Glycinin in 8M Urea or 6M Guanidine Hydrochloride Solution. *J. Agric. Food Chem.* **1984**, *32*, 1402–5.

Thanh, V. H.; Shibasaki, K. Major Proteins of Soybean Seeds. A Straightforward Fractionation and Their Characterization. *J. Agric. Food Chem.* **1976**, *24*, 1117-21.
Thanh, V. H.; Shibasaki, K. Beta-conglycinin from soybean proteins. Isolation and immunological and physicochemical properties of the monomeric forms. *Biochim. Biophys. Acta* **1977**, *490*, 370-84.
Thanh, V. H.; Okubo, K.; Shibasaki, K. Isolation and Characterization of the Multiple 7S Globulins of Soybean Proteins. *Plant Physiol.* **1975**, *56*, 19.
Utsumi, S.; Kinsella, J. E. Forces Involved in Soy Protein Gelation: Effects of Various Reagents on the Formation, Hardness and Solubility of Heat-induced Gels made from 7S, 11S and Soy Isolate. *J. Food Sci.* **1985**, *50*, 1278-82.
Wüthrich, K. Carbon-13 NMR of Amino Acids, Peptides and Proteins. In *NMR in Biological Research: Peptides and Proteins*; North-Holland/American Elsevier: Amsterdam, Oxford, New York, 1976.
Yamauchi, F.; Yamagishi, Y. Carbohydrate Sequence of a Soybean 7S Protein. *Agric. Biol. Chem.* **1979**, *43* (3), 505-10.

Received for review November 15, 1988. Revised manuscript received August 29, 1989. Accepted December 14, 1989.

# Effect of Structural Constituents of Cell Wall on the Digestibility of Grape Pomace

Oluyemi O. Famuyiwa and Cornelius S. Ough*

Department of Viticulture and Enology, University of California, Davis, Davis, California 95616

In vitro dry matter digestibility, cell wall digestibility, and chemical composition of cell solubles and cell wall fractions were determined from three grape pomace varieties and two standard feeds. Dry matter digestibility of pomace was low (25–38%) compared to standard feeds. Cell solubles content of pomace is comparable to that of standard feeds but is comprised of organic acids (tartaric and acetic) and pectic polysaccharides. Cell wall digestibility of Cabernet Sauvignon pomace is very low (4%), and lignin + cutin level is very high (29%) compared to standard feeds (34–42% and 6–8%, respectively). The observed digestibility is explained in terms of the structural composition of the cell wall fraction.

Previous investigations have revealed that winery pomace is high in crude fiber and low in digestibility (Folger, 1940; Leonard et al., 1978). Since the nutritional value of a feed depends on its chemical composition, chemical analyses are important in explaining observed nutritional properties of feeds. The detergent system of analysis (Goering and Van Soest, 1970) has been used to quantitatively determine cell wall, cellulose, hemicellulose, and lignin + cutin content of feeds. On the basis of this, digestibilities of forages could be predicted and causatively related (Mowat et al., 1969; Smith et al., 1972; Robbins et al., 1975). From an enological perspective, methods of fractionating grape pulp and skin polysaccharides were developed to provide a better understanding of the biochemistry of wine making (Ezhov and Datunashvili, 1974; Zinchenko et al., 1975; Morgues, 1979). In this report, grape pomace was fractionated with use of modifications of both extraction techniques. Some of these fractions were chromatographically analyzed, and the information obtained is used to explain the observed low in vitro digestibility figures.

## MATERIALS AND METHODS

**Grape Pomace Varieties.** Cabernet Sauvignon (CBS), Gewurtztraminer (GWZ), and Tinta Madeira (TMD) were obtained fresh from wineries in Northern California. The seeds were manually removed and the skins dried in a blown-air oven at 60 °C for 48 h and ground in a Willey mill fitted with a 1-mm screen.

**Standard Feeds.** Alfalfa hay mixed with grain and Sudan grass hay were obtained from the Nutrition Laboratory of the Animal Science Department of UCD.

**In Vitro Dry Matter Digestibility (IVDMD).** This was determined by the two-stage technique of Tilley and Terry (1963) using rumen fluid obtained from cow, sheep, or goat.

**In Vitro Cell Wall Digestibility (IVCWD).** This was determined as above, but the starting material was the cell wall fraction, obtained by refluxing the feed in neutral detergent solution.

Detergent extraction was performed according to the method of Bailey and Ulyatt (1970), incorporating sequential analyses (Figure 1). Grape skin polysaccharides were fractionated according to Figure 2.

**Analysis of Fractions.** Uronide content was determined with *m*-hydroxybiphenol (Ahmed and Labavitch, 1977). Organic acids were determined by high-pressure liquid chromatography (Heymann, 1980), and neutral sugars were determined by gas–liquid chromatography according to Ahmed and Labavitch (1980).

## RESULTS AND DISCUSSION

All the pomace samples had low IVDMD compared to the standard feeds (Table I). CBS pomace had higher digestibilities than the other pomace varieties irrespective of the source of rumen fluid, but it was still about 30% lower than the standard feeds. CBS pomace was favored over the others because the grapes are uniformly treated in all wineries, resulting in a pomace of

0021-8561/90/1438-0966$02.50/0 